IAC-24-D4.5.5

Experimental Demonstration of the Electrochemical Reduction of a Lunar Highland Simulant to Metallic Aluminum. Factors Affecting the Reactor's Performance

Xavier Walls [a,] *, Alex Ellery [b], Priti Wanjara[c], Katherine Marczenko[d]

[a] *Department of Mechanical and Aerospace Engineering, Carleton University, 1125 Colonel By Drive, Ottawa, ON, Canada. K1S 5B6,*
Aerospace Research Centre, Aerospace Manufacturing Technology Centre, National Research Council, 2107 chemin de la Polytechnique (Campus de l'Université de Montréal), Montréal, QC, Canada. H3T 1J4, xavierwallsperez@cmail.carleton.ca
[b] *Department of Mechanical and Aerospace Engineering, Carleton University, 1125 Colonel By Drive, Ottawa, ON, Canada. K1S 5B6,* alexellery@cunet.carleton.ca
[c] *Aerospace Research Centre, Aerospace Manufacturing Technology Centre, National Research Council, 2107 chemin de la Polytechnique (Campus de l'Université de Montréal), Montréal, QC, Canada. H3T 1J4,* priti.wanjara@cnrc-nrc.gc.ca
[d] *Department of Chemistry, Carleton University, 1125 Colonel By Drive, Ottawa, ON, Canada. K1S 5B6,* katherinemarczenko@cunet.carleton.ca
* Corresponding Author

Abstract

Aluminum has been a staple material for the aerospace industry. Its adoption enabled the construction of lighter and more efficient structures due to its excellent strength-to-weight ratio. Humankind is getting closer to returning to the lunar surface every day. Unlike previous missions, everything seems to point out that this time humans will arrive to stay there. A sustained presence on the Moon will require a continuous supply of resources. Aluminum will surely be one of the fundamental resources for humans on the Moon as this element is widely available in lunar anorthite. The extraction of this element and any other extraterrestrial resource should be based on sustainable mining. Any waste should be minimized, and resources should be recycled and reused. The feasibility of extracting alumina from a lunar highlands' regolith simulant has been previously demonstrated. The objective of this work is to provide an insight into the factors that impact the operating efficiency of a bench-scale electrochemical reactor capable of reducing alumina to metallic aluminum. A cooling system was used to prevent any damage to the plugs and tubing. The electrolyte was dehydrated to prevent any interactions between the aluminum produced and water. A stainless steel rod with a graphite block inserted in it was used to replace a pure carbon anode which was prone to additional corrosion in the headspace. Best results were obtained when using solid alumina pellets with a wide opening. Conductive graphite and metallic calcium were used as additives for the electrolyte to increase the conductivity and increase the rate of reduction. It was possible to produce aluminum spherules with a purity of around 99% according to x-ray diffraction (XRD) and energy dispersive X-ray spectroscopy (EDS) analyses. Aluminum obtained from the process was used to produce a wire that is intended for further testing using electron beam additive manufacturing (EBAM). A basket electrode was also used to electrolyze a beneficiated lunar highlands' simulant (LHS-1) sample. The large contact surface of this electrode increased the current density resulting in the loss of electrolyte. Stainless steel has a poor performance in this process. Any produced aluminum will immediately fuse with iron creating openings through which reagent particles can go through. Some particles in the beneficiated LHS-1 were successfully reduced. The results of EDS mapping showed the presence of particles composed of aluminum lightly combined with calcium, with a practically null amount of oxygen and a minimum silicon content.

Keywords: (Aluminum, Electrochemistry, Moon, Space Resources, Molten Salt Electrolysis, ISRU)

1. Introduction

Aluminum (Al) is a critical element for the aerospace industry, where it has been a staple material since the 20th century. Its adoption revolutionized this industry by enabling the construction of lighter and more efficient aircraft due to its excellent strength-to-weight ratio. Its lightweight nature helps in maximizing the payload capacity and improving the overall fuel efficiency of spacecraft. This element offers other excellent properties such as the ease of machining, which allows the precise production of complex components such as spacecraft, and structural frames. Al also offers good resistance to corrosion, which is particularly beneficial for spacecraft operating in harsh environments including space and atmospheric re-entry. The ability of this element to withstand these conditions without significant degradation ensures the reliability and longevity of space missions.

Humankind is getting closer to returning to the lunar surface every day. Unlike previous missions, everything seems to point out that this time humans will arrive to stay there. A sustained presence on the Moon would require a continuous supply of resources. So far, most of the research has focused on the extraction of essential resources for human survivability, such as water. However recent studies have shown that the extraction of this resource presents major challenges that have yet to be solved. We propose that the efforts should be focused first on resources that are more accessible and widely distributed on the lunar surface. An element that perfectly fits these criteria and that would be very useful for a sustained human presence is Al.

The lunar surface is mainly comprised of only a few minerals: feldspar, olivine and pyroxene. Most of the lunar feldspar found on the Moon is part of plagioclase series, which ranges from the sodium-rich albite ($NaAlSi_3O_8$) to the calcium-rich anorthite ($CaAl_2Si_2O_8$). Since the Moon has a deficiency of alkali elements, albite is relatively rare, whereas anorthite is prevalent [1]. The two main regions on the Moon: Mare and Highlands have a slightly different mineralogical content. Lunar Mare is mostly made of basaltic rock, while the Lunar Highlands are mostly composed of anorthositic rocks. Despite this difference, both regions share a high abundance of this material. It is estimated that overall, the lunar surface is composed of about 83% anorthositic material [2].

As of today, lunar regolith (particularly from the highlands) is probably the major mineral deposit on the Moon. Because of its high anorthite content, the regolith is a valuable reservoir of highly useful elements for a prolonged human presence on the Moon. A few techniques have been proposed with the aim of extracting these resources, the most popular ones so far are Molten Regolith Electrolysis (MRE), and Carbothermal Regolith Reduction (CRR).

MRE is an electrochemical technique where the lunar regolith (containing a series of metallic oxides) is heated to extremely high temperatures, typically over 1600°C until it becomes a molten liquid [3]. Once the regolith is molten, a couple of electrodes are introduced in it, and an electric current is passed through. In this process, metals are produced at the cathode and oxygen (O_2) is released at the anode. The main advantage of MRE is its ability to efficiently extract O_2 and other metals, such as calcium (Ca) or Al from the lunar regolith simultaneously without the need of water or any electrolyte. However, the implementation of MRE also faces great challenges. The process requires substantial amounts of electrical energy to maintain the high temperatures required to keep the regolith in a molten state and to drive the electrolysis reaction. Managing the high temperatures of molten regolith can be technically challenging, requiring robust and durable materials for the infrastructure, which would be difficult to be sourced from the Moon. Additionally, it is possible that the high density and viscosity of the molten regolith may affect the release of the O_2 produced by MRE under low-gravity lunar conditions [4].

CRR is a chemical process where the lunar regolith is mixed with a carbon (C) source such as coke or graphite. The mixture is heated at extremely high temperatures of about 1600°C. At these high temperatures, C reacts with the metal oxides in the regolith reducing them into metals releasing carbon dioxide (CO_2) as a byproduct [5]. The main advantage of this process is that like MRE, all the oxidized regolith components can be reduced in a single step. Additionally, the CO_2 could be electrolyzed to C and O_2. This would allow C to be reused in the CRR process and O_2 to be used for habitation or transportation purposes. There are also significant challenges associated with this process. Similar to MRE, it would require materials capable of maintaining the high temperatures required for the process. However, the main problem would be ensuring a consistent supply of C. This material is scarce on the Moon, and it would have to be transported from Earth, unless a local resource is found on the Moon, or if human C waste could be transformed into elemental C to be used by the CRR process. The best way to separate the outputs of these processes remains to be studied. Since different elements are present in the regolith, a mixture of metals or a series of alloys would be expected. In addition, the by-product would be expected to be mixed with the products forming a “slag”. The Marangoni effect has been proposed for this purpose, however, there’s currently no system in existence with the capacity of separating the different elements that would be present in this kind of “slag”.

We propose that the procedures commonly used on Earth for the extraction of a particular resource should also be adopted on the Moon for the extraction and utilization of resources. The mining industry is one of the oldest human activities, traced back to more than 40,000 years. Throughout this time, several key lessons have been learned, reflecting both progress in technology and growing awareness of environmental and social impacts.

With the evolution of mining, a series of processes have been commonly adopted and followed to ensure that a desired resource is obtained:

1. Crushing and Grinding: The ore is broken into smaller pieces to increase the surface area for further processing. Grinding the material into a fine powder usually helps to release the valuable minerals.
2. Concentration or beneficiation: Valuable minerals are separated from undesired material through a series of techniques such as gravity separation, flotation, or magnetic separation.

3. Leaching: The ore or concentrate is treated with chemical solutions to dissolve the target mineral where the desired metal is present.
4. Separation and Extraction: The desired metal (usually in the form of ions) is selectively extracted from the leach solution by techniques such as precipitation, drying, solvent extraction, or ionic exchange.
5. Refining and Purification: The metal is recovered, and any impurities are removed. This is usually achieved through electrolysis and electrorefining.

According to the above processes it is normally easier to remove any potentially unwanted material during the early stages of the process. We suggest these steps should be implemented on the extraction of space resources.

Early mining on Earth often ignored the environmental consequences of this practice. Modern practices emphasize rigorous environmental impact assessments and mitigation strategies to manage pollution, environmental destruction, and waste. Sustainable mining must be implemented in any type of mining, whether inside or outside our planet. Any waste should be minimized, the efficiency of resources should always be considered, and practices that ensure the long-term viability of the process should be prioritized. A circular economy should revolve around any extraterrestrial resource, where efforts are made to recycle and reuse materials to reduce reliance on new or unexpected resources.

On Earth, Al extraction in achieved through two critical processes: the Bayer process, and the Hall-Héroult (HH) process. The Bayer process is the primary method used to obtain alumina (Al_2O_3), while the HH process is the primary method for producing Al metal from Al_2O_3. While these processes are highly efficient and have become a standard practice for the Al industry, they are not a viable alternative on the Moon. The Bayer process uses bauxite as feedstock, but Al on the Moon is available in the form of anorthite. The Bayer process also requires a significant amount of water for the precipitation and washing stages but water on the Moon is extremely scarce; any existing water is trapped in permanently shadowed craters as ice or chemically bound in minerals. Flocculants are also used in the Bayer process; the most common one is polyacrylamide [6], which is derived from petrochemical sources on Earth. Ensuring a continuous supply of this flocculant on the Moon would be challenging. The HH process uses cryolite (Na_3AlF_6) as the electrolyte. Sourcing Na_3AlF_6 would present significant challenges on the Moon. There are no known natural deposits of Na_3AlF_6 on the Moon and producing it synthetically would be limited by fluorine (F), a very scarce element on the Moon. Also, the HH process prefers C as a material for the electrodes. As C is practically absent on the Moon, it would need to be sourced from Earth.

A viable alternative to the processes that have previously been proposed for harvesting lunar resources (MRE and CRR) is based on the two-step terrestrial Al mining. The Bayer process is replaced with a process in which the regolith is beneficiated by magnetic separation followed by acid leaching. Al_2O_3 was successfully obtained by this process [7]. The average purity of the Al_2O_3 produced by this type of acid leaching is usually around 95% [8]. In the present work, the results of the second part of the process are presented. The HH process was replaced with an adaptation of the Fray, Farthing, Chen (FFC) process [9], both processes fall into the category of Molten Salt Electrolysis (MSE) as a molten electrolyte is used to facilitate the current flow inside of the reactor. In the FFC process the cathode typically either contains or it's made from the metallic oxide to be reduced (typically TiO_2). Al_2O_3 is used in these experiments. Another difference to the HH process is that calcium chloride ($CaCl_2$) is used as the electrolyte in the FFC process, while Na_3AlF_6 is used on the former.

The method being proposed adheres to the principles of sustainable mining and circular economy, where the supply from Earth-imported materials and the range of exploited materials on the Moon is minimized [10]. During the initial step of the process, the only reagent that would be imported from Earth is hydrochloric acid (HCl) which would be used to leach beneficiated lunar regolith at relatively low temperatures (95°C – 100°C):

$$\mathrm{CaAl_2Si_2O_8 + 8HCl + 8H_2O \rightarrow CaCl_2 + 2AlCl_3 \cdot 6H_2O + 2SiO_2}$$

Silica (SiO_2) precipitates and is separated as a subproduct, while $CaCl_2$ and aluminum chloride hexahydrate ($AlCl_3 \cdot 6H_2O$) remain in solution after leaching. $AlCl_3 \cdot 6H_2O$ can be then precipitated through sparging and separated from the solution, resulting in two distinct fractions of $CaCl_2$ in solution and $AlCl_3 \cdot 6H_2O$ as a solid. The $AlCl_3 \cdot 6H_2O$ can be decomposed by heating to approximately 100°C to produce Al_2O_3:

$$\mathrm{2AlCl_3 \cdot 6H_2O \rightarrow Al_2O_3 + 6HCl + 9H_2O}$$

As shown in this reaction, HCl is one of the products of the decomposition of the $AlCl_3 \cdot 6H_2O$. This opens the possibility for HCl to be collected and reused in the leaching step. Additionally, the process would produce a minimal amount of waste since practically all the produced material would have an application on the moon. The iron-rich magnetically separated fraction could be processed into iron (Fe) by carbothermal reduction, the thermite reaction, or by molten oxide electrolysis. SiO_2 could be used to make cement, ceramics, fire bricks, glass, microchips, optical fiber, among others. SiO_2 could also be reduced into elemental silicon (Si), which would be useful for making different alloys on the Moon, to produce integrated circuits, semiconductors, solar cells, etc. $CaCl_2$ could be used as a water absorbent, as a desiccant, as a de-icing agent, or even for a lunar food industry. However, we propose that the most important application for the produced $CaCl_2$ would be to be used as the electrolyte for the electrochemical reduction of Al_2O_3 into metallic Al.

The MSE process proposed based on the FFC [11] maintains the supply chain by using the Al_2O_3 produced from the leaching step as feedstock for the reaction while $CaCl_2$ is used as the electrolyte. Additionally, the MSE process is more energy efficient than MRE and CRR because it takes place at a much lower temperature of between 900°C – 1100°C, while MRE and CRR take place at higher temperatures of between 1500°C – 2000°C. This process also presents itself as an alternative in which the electrodes could be made of a non-carbon material, which poses a significant advantage to CRR. The use of an inert material anode would also allow the recovery of the O_2 released from the reaction. The viability of MSE has already been demonstrated on the direct electrolysis of a JSC-2A simulant where the authors demonstrated it was possible to recover 96% of the O_2 present in the regolith [12], however, the authors didn't focus on selectively extracting a specific solid resource from the regolith.

In this paper, the successful deoxidation of Al_2O_3 into metallic Al by MSE is demonstrated. An insight into the factors that impact the reactor's operating efficiency is also provided. The influence of some factors on the resulting Al is also discussed. Manufacturing of Al Wire feedstock for an additive manufacturing system that uses an electron beam is also shown.

2. Material and methods

The first component considered for the reactor was the heating device. An electrically heated kiln-type furnace was selected to achieve the necessary temperatures for the reaction (900°C – 1100°C). The furnace has a cylindrical heating chamber located on the centre of the furnace with a type-K thermocouple located inside.

A custom-made 304 stainless steel retort with a lid was manufactured to be placed inside the heating chamber. The lid was designed to insert 5 fittings. The elements placed on each of the fitting were: a gas inlet, a gas outlet, a K-type thermocouple to record the temperature while the reaction was taking place, a cathode and an anode. An Al_2O_3 crucible was placed inside of the retort to prevent interactions with the stainless steel as best as possible.

An Argon (Ar) cylinder Linde grade 4.8 (99.998% purity) was used for the reaction to take place in an inert atmosphere. Silicone tubing was used to connect a Schlenk line directly to the fitting on top of the retort lid. Experiments were performed with and without an inert atmosphere.

Different electrode configurations and materials were tested C (conductive graphite), stainless steel, and molybdenum (Mo) were the materials used for the cathode. Basket and rod shapes were used. Three different configurations were used for the anode: solid stainless steel rod, solid conductive graphite rod, and a stainless steel rod with a conductive graphite block.

99.9% pure Al_2O_3 pellet samples and an LHS-1 regolith simulant were used as reagents for the experiments. The reagents were introduced into the electrodes for testing.

The electrodes and thermocouples used for the experiments were protected with high temperature resistant sleeves. The sleeved electrodes were secured onto the reactor using silicone plugs. A recirculatory system and a heat shield were used to decrease the temperature of the lid and protect the silicone plugs and tubing. The recirculatory system was comprised of a recirculatory water bath kept at 25°C, silicone tubing and a copper coil that was manufactured to surround the reactor lid to preserve the integrity of the electrodes, silicone tubing, and silicone plugs.

Calcium chloride dihydrate ($CaCl_2{\cdot}2H_2O$) Sigma-Aldrich ReagentPlus (99.99%) was used as the electrolyte for the reaction. $CaCl_2$ is highly hygroscopic and is commercially available in various hydration states: anhydrous, dihydrate, tetrahydrate and hexahydrate. The anhydrous version is very costly to acquire. The dihydrate version was selected as a cost-effective option. The creators of the FFC process also preferred $CaCl_2 \cdot 2H_2O$ over the anhydrous option. Their heating procedure of increasing the temperature from 20 to 300°C at a rate of 300°C/h, holding at 300°C for 6 h or longer, then heating it under Ar to 700°C, and maintaining the temperature for a couple of hours before the reaction [13] was tested. Then further experiments were conducted to remove as much as water as possible from the electrolyte to see if it would improve the results.

The voltage was varied in 1V increments to see if there was any effect on the electrolyte, the electrodes or the final product. Any products obtained from the process were washed with deionized water and ultrasonically cleaned until any salt was completely removed. More details on the construction of the reactor and some initial results can be found in [14].

The samples were analyzed by XRD using a Malvern Panalytical Empyrean Diffractometer. Additional images were taken by scanning electron microscopy (SEM). Qualitative elemental analysis results were obtained through energy dispersive X-ray spectroscopy (EDS). Some samples had to be mounted in non-conductive epoxy resin (Buehler EpoThin 2). The surface was then ground and polished to obtain a mirror-like finish. Any samples analyzed by SEM and EDS were coated with C (conductive graphite). The microscope used was a Tescan Vega-II XMU Scanning Electron Microscope, and the detector used was an Oxford Inca Energy X-Act EDS detector.

Finally, an Al wire was fabricated with the reaction products. A sample of the Al produced was poured into a cylindrical mold. The surface of the Al cylinder was sanded and blown with a hammer. After that, it was rolled several times until the diameter was small enough to go through a wire drawing process. One of the tips was sanded and inserted into a tungsten carbide die which was lubricated with a molybdenum disulfide (MoS_2) lubricant. The Al was subsequently drawn with a mechanical system using pliers. The process was repeated several times using a smaller die each time until getting the diameter required for an EBAM system (between 1.6 mm and 0.9 mm). The wire was softened through an annealing process at 350°C whenever the Al became difficult to draw.

3. Results and Discussion

1.1 Improving the reactor.

The first efforts were focused on protecting the material of the plugs, electrode sleeves, and tubing from the high temperatures of the process. Two options were selected for this purpose, a heat shield and a recirculatory cooling system. The heat shield (Fig. 1) was made with a stainless steel disc bored with 3 holes: two for the electrodes and one for the thermocouple. The recirculatory cooling system had three elements: a recirculatory water bath, silicone tubing and a copper coil. The tests were performed with copper tubing with different diameters (3/8 in, ¼ in, and 1/6 in). As shown in Fig. 2, the copper tubing could wrap more times around the reactor lid as the diameter of the tubing decreased with the 3/8 in, 1/4 in and 1/6 tubes wrapping three times, four times and five times around the lid, respectively.

Two thermocouples were installed to verify the efficiency of the heat shield and the recirculatory cooling system. The first thermocouple used was short-length and was only in contact with the lid. The second thermocouple was longer and was immersed in a crucible with $CaCl_2$ located inside the retort.

The results revealed that on average the use of the recirculatory cooling system placed on the lid lowered its temperature by between 350°C to 550°C. The coil that yielded the best results was the one made with 1/4 in tubing decreasing the temperature by around 550°C. It was followed by the 3/8 in tubing where the lid's temperature was decreased by around 385°C. The one that showed the worst results was the 1/6 in tubing, where the temperature was only decreased by around 350°C. The use of the heat shield did not significantly affect the results. If the reactor was used for a short period of time (between one and three hours), the heat shield helped to decrease the lid temperature by about 200°C over the temperature achieved by the recirculatory cooling system. However, after that period of time, the lid temperature started to increase until it stabilized at the same temperature reached by using the recirculatory cooling system alone. This suggests that after a certain period of time, the stainless steel heat shield eventually became hot enough to allow some heat transfer to the lid. It is possible that using another material may improve its efficiency, however, this was not tested in this work.

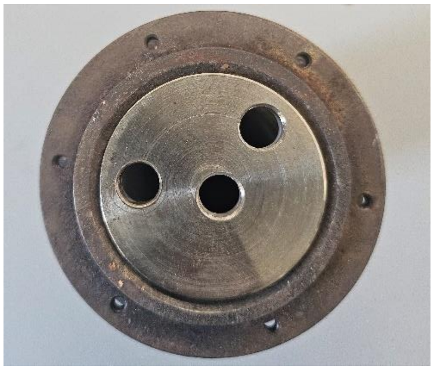

Fig. 1. Top view of the retort and the stainless steel heat shield. The heat shield is shown in the centre in a lighter colour. The heat shield has three holes for the two electrodes and a thermocouple and covers the heating enclosure preventing heat from reaching the lid.

Fig. 2. Copper coils used for the cooling system. Copper tubing of different diameters is shown (3/8in, 1/4in, and 1/6 in from left to right). As the diameter of the tubing decreases, it can coil more times around the lid.

Fig. 4 shows the difference between the retort body and the lid. It can be clearly seen that the vessel shows a change in coloration as a result of the heating experienced by the vessel. In contrast, the lid maintained its integrity thanks to the cooling system. The lid kept its original colour, and no signs of damage were observed. The last test was carried out using silicone tubing in the gas inlets to test if the material could withstand the final temperature set on the lid by the cooling system. It was possible to maintain a lid temperature of 400°C, while the internal temperature of the reactor was 950°C (temperature at which the reaction takes place). The silicone tubing successfully withstood this temperature. The use of a heat shield was abandoned as it did not significantly improve the cooling of the lid and would interfere with the handling of the electrodes and the thermocouple.

Fig. 3. Cooling system testing. The image shows the cooling system featuring copper tubing during one of the initial tests with the 3/8-inch copper tubing coil around the lid. Two thermocouples are located on the top of the lid. The one located at the back is a long thermocouple that is immersed in the retort, while the thermocouple located at the front is just a superficial thermocouple which is only in contact with the lid.

Fig. 4. Coloration contrast between the retort body and lid post-heating. This image shows the difference in coloration between the retort body and the lid after heating. The vessel shows clear signs of heat exposure, while the lid remains undamaged due to the cooling system, preserving its original color.

The second test performed was aimed to remove as much water as possible from the electrolyte ($CaCl_2 \cdot 2H_2O$). To do this, the method used by the authors of the FFC process was first tested. Then, different temperatures and heating times were tested. Also, a vacuum furnace was used to test a simultaneous heating and reduced pressure process. Fig. 5 shows the diffractogram of the different heating processes. Fig. 5A shows the pattern of the $CaCl_2 \cdot 2H_2O$ pure reagent. It was used as a reference to analyze the efficiency of each process. The three main peaks of the dihydrate version are located at around 9.5°, 21°, and 34°. Fig. 5B shows the diffractogram of a $CaCl_2 \cdot 2H_2O$ sample heat treated by the procedure chosen the authors of the FFC process: heating at 300 °C for 6 h or longer, and then heating it under Ar to 700°C, and maintaining the temperature for a couple of hours. The values obtained by the Rietveld method indicated a $CaCl_2 \cdot 2H_2O$ to $CaCl_2$ transformation of 41%. This was the highest value achieved by this treatment. Experiments were performed by holding the temperature over a longer period of time, however, no major change in the composition was observed after heating for 8 hours, which is represented on Fig. 5B. Fig. 5C shows the diffraction pattern after incorporating vacuum to the heating method. The sample was heated to 300°C for 6 hours and then allowed to cool down to 125°C. At this temperature, the vacuum pump was turned on for 3 hours reaching a pressure of 12 inHg. It can be observed that the incorporation of vacuum was successful. It was possible to obtain about 19% more of the dehydrated phase. Finally, Fig. 5D. shows the best results obtained in this study. The diffraction pattern shown is a result of $CaCl_2 \cdot 2H_2O$ heated at 300°C for 6 hours and then decreasing the temperature to 225°C. At this temperature the vacuum pump was turned on and maintained for 8 hours reaching a pressure of 12 inHg. It can be observed that up to 84% of the dihydrate phase could be removed.

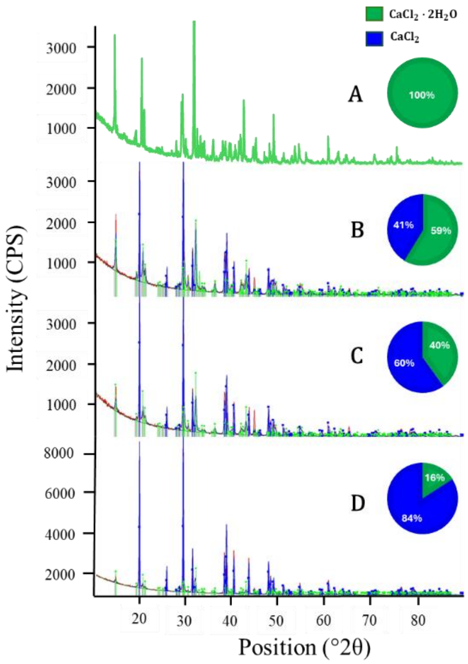

Fig. 5. Heating treatment of $CaCl_2 \cdot 2H_2O$. Fig. 5A shows the pattern of the $CaCl_2 \cdot 2H_2O$ pure reagent. Fig. 5B shows the pattern $CaCl_2 \cdot 2H_2O$ after testing the heat treatment by Chen & Frey [13]. Fig. 5C shows the pattern after a heat treatment of 300°C for 6 hr and 3 hr vacuum at 125°C. Fig. 5D shows the pattern after a heat treatment of 300°C for 6 hr and 8 hr vacuum at 225°C.

Looking at the main peaks of $CaCl_2 \cdot 2H_2O$ across the different experiments, it is clear that the intensity decrease of the peaks associated to $CaCl_2 \cdot 2H_2O$ is proportional to the percentage of water removed. Similarly, the increase in the intensity of the main signals of the dehydrated $CaCl_2$ at 19.5°, 28° and 37° increases as the water content decreases. If a comparison is made between Fig. 5A and Fig. 5D, it can be clearly seen that the diffraction patterns are completely different.

According to Chen and Fray's experiments [13] they were able to get successful results in the reduction of rutile (TiO_2) with the less exhaustive heating procedure. We decided to further decrease the water content in the $CaCl_2$ because Al has a high affinity for hydrogen and it's also prone to oxidation. It is usually desirable to remove the presence of any hydrogen source as it causes imperfections in the Al by causing porosity. We theorized that by decreasing the hydration level of the electrolyte, better reaction results could be possible and at the same time better quality Al.

Finally, the method selected for the electrolysis experiments was to melt pre-dehydrated $CaCl_2$ by this method at 800°C, until the Al_2O_3crucible was filled to the top, leaving only room for the electrodes and thermocouple. After that, the retort was covered with the lid containing the electrodes and thermocouple. Only the thermocouple was submerged into the molten salt. The lid was sealed, and the cooling coil was placed surrounding it. The recirculatory system was activated. The silicone tubing for the gas inlet and outlet was connected and Ar was allowed to flow into the reactor. The temperature of the molten $CaCl_2$ was maintained at 800°C and Ar kept flowing for a couple hours to remove any water that could have been absorbed during the handling. Following this period, the temperature was ramped up to 950°C and the two electrodes were submerged into the molten electrolyte and connected to a power source ramping up the voltage.

1.1 Factors influencing the experimental results.

Once everything was ready to perform the reaction, a series of tests were conducted to ensure that the process was successful. The first issue faced was the behavior of the graphite anode. It was impossible to run the reaction for long periods of time. It was observed that by holding the voltage constant, the current would decrease as time went by until it reached a point where the current was zero. After testing different hypotheses, it was concluded that the decrease in current and the fact that it reached zero was due to the deterioration of the graphite electrode, which eventually broke. This conclusion was reached after finding several graphite tips (Fig. 6) immersed in the solidified electrolyte from several attempted reactions. This indicates that the tip of the electrode is not the part that suffers the most corrosion and that there's a secondary reaction happening in the headspace between the electrolyte and the lid. It is well known that graphite and O_2 react spontaneously at high temperatures [15] and that the reaction becomes more pronounced as the temperature increases. Thus, in addition to the electrochemical reaction happening in the anode, there is also a reaction happening between gaseous O_2 and C from the graphite electrode.

Fig. 6. Damaged graphite electrode. The picture shows a tip which was found in the solidified electrolyte indicating corrosion of the graphite rod and suggesting a reaction between graphite and oxygen in the headspace.

Fig. 7 shows the type of deterioration observed in the electrode and the solution to that issue. Fig. 7A shows how the graphite electrode suffers from additional corrosion in the section between the electrolyte and the lid. The diameter of the graphite rod constantly decreased until it reached a point where the electrode broke, and the tip fell into the electrolyte. Fig. 7B shows the electrode designed to prevent those fractures. The electrode consisted of a stainless steel rod in which a graphite block was inserted. To achieve a successful reaction, the graphite section was completely submerged in the electrolyte.

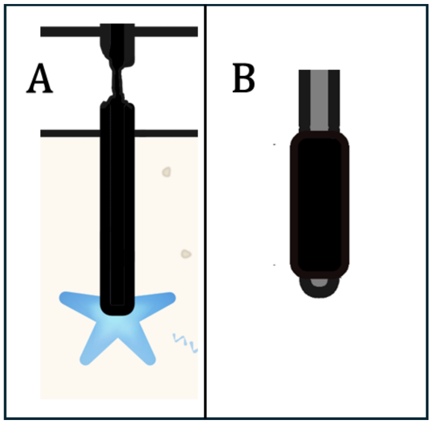

Fig. 7. Corrosion of the graphite electrode and improvement to the design. Fig. 7A shows the type of corrosion observed in the space between the electrolyte and the lid. The graphite rod got thinner until it reached its breaking point. Fig. 7B shows a new design for the graphite electrode. It was made with a stainless steel rod where a graphite block was inserted.

Another factor considered in the experiments was the type of reagent to be used. The Al_2O_3 obtained from the LHS-1 lunar regolith simulant was in the form of a powder [7]. However, it has been studied [16] that this is not very efficient because the reduction of Al_2O_3 occurs at the three-phase zone where O^{2-} ions are produced. The diffusion of these ions is slow in powdered Al_2O_3 due to the small space among particles. It was decided to use a center-holed pellet instead of powder to allow better diffusion the diffusion of O^{2-} ions.

Fig. 8 shows the first promising results. The walls of the Al_2O_3 pellet were coated with a metallic Al finish. However, it was not possible to cover the whole pellet or to transform all the material into Al. This problem is probably associated to the diffusion of the O^{2-} ions since, despite having chosen a bored pellet, the hole was only large enough for the electrode to pass through. To improve the results, the diameter of the hole was widened to facilitate the diffusion. Fig. 9 shows the hole widening and a cross section of the pellet to depict the diffusion happening there. The widening of the hole facilitates the diffusion of the O^{2-} ions because it provides them a path to migrate away from the electrode. Also, any O^{2-} ions generated from the reduction of Al_2O_3 occurring inside the hole can diffuse out.

The widening of the pellet hole made it possible to reduce Al_2O_3 more efficiently. Fig. 10 shows the formation of a few Al spheres. However, they were very small and most of the Al_2O_3 pellet remained attached to the electrode.

Fig. 8. Al_2O_3 pellet coated with Al after the electrochemical process. The image shows early promising results. A metallic coating was formed around the pellet. Only the outside of the pellet had a metallic finish, while the body of the pellet was unchanged.

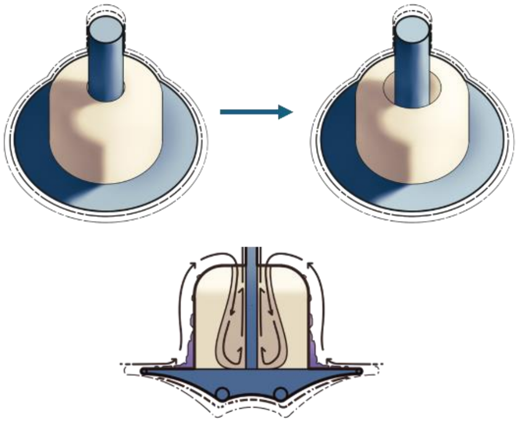

Fig. 9. Widening of the Al_2O_3 pellet and diffusion path of the O^{2-} ions. The upper images show the difference between the first pellet used (left) compared to the pellet with the amplified hole (right) to facilitate diffusion of the O^{2-} ions. The image at the bottom shows the ion diffusion path. It is also shown that the ions forming within the hole can also flow out easily.

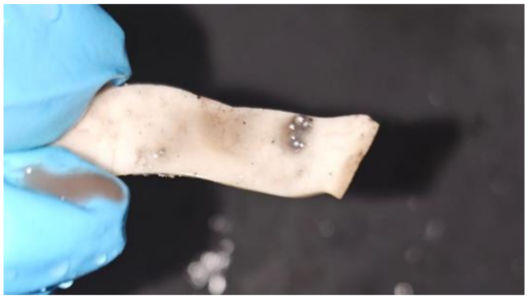

Fig. 10. First Al spheres obtained from the reaction. The pictures show the first Al spheres that were detached from the Al_2O_3 pellet. The spheres were very small and were found while rinsing the reaction products with deionized water.

The voltage was varied in 1 V increments from 1 to 5 V to determine the ideal voltage for the process. The minimum voltage determined to be required to start the process was between 2.8 – 3.2 V, however best results were achieved using voltages in the order of between 4 – 5 V. Most successful results were obtained by ramping up the voltage to 4.5 V to start the reaction and overcome the activation energy. Once there was a drop in current, the voltage was kept constant at 4.1 V. The use of a higher voltage to start the reaction was important to get good results, as it drove the rapid formation of a variety of active nucleation sites at the start of the process where the reduction reaction would take place simultaneously. The voltages used in this study are similar to the ones used for the HH process which range from 4 – 5V. It should be noted that the best voltage for each reactor depends on a wide set of variables and that's the main reason for the wide range of voltages used by the HH process. Some of the factors that affect the voltage in an individual reactor are the use of different electrode materials because each material has a different resistance. This is particularly important for O_2 evolution. It is possible that replacing a graphite electrode for an inert anode to produce pure O_2 will change the voltage requirements significantly. Additionally, the deterioration of the electrodes will have an overvoltage effect on the process, for example a reused electrode will probably have a rougher surface, and the overvoltage needed to drive the reaction will probably increase. The aging of any components in the cell, such as the cell walls, will also lead to higher overvoltages. The conductivity of the electrolyte will also change the voltage required to drive the reaction. The conductivity of molten electrolytes (such as the $CaCl_2$ we used), typically varies depending on its temperature. A change in temperature changes its density and viscosity, factors that can also affect the diffusion of ions in the melt. Also, the presence of water in the electrolyte and the formation of a small amount of CaO during the process can affect the conductivity of the electrolyte. It should be noted that the bench scale reactor was very small allowing the electrodes to be placed close to each other. However, it's possible that scaling up the process will require a higher voltage because the distance between the electrodes will increase, causing some significant resistive losses.

Fig. 11. Al spherules obtained from the electrochemical process. The spherules are placed in a sample holder. These spheres were the result of the best parameter optimization achieved so far. The increase in size is considerable with respect to the spheres of Fig. 10.

A few additional enhancements to the performance of the reaction were to add some conductive graphite powder to the electrolyte to improve the conductivity inside the cell. 4% Ca metal was added as an additive. It's addition as an additive improves the performance of the calicothermal mechanism of the electrolyte where elemental Ca can sequester O_2 from the Al_2O_3 forming calcium oxide. The oxide is highly soluble in $CaCl_2$ preventing any layer of oxide from forming around the electrodes. Additionally, a part of the calcium oxide formed can be re-dissociated [17]. Fig. 11 shows some of the Al metal spherules that were obtained after the optimization of all the previously mentioned parameters.

Fig. 12 shows the analysis results of the Al samples using XRD and EDS. Fig. 12A shows the XRD pattern of the Al produced. The peaks observed in the diffractogram are characteristic to Al. The Rietveld analysis results showed an Al content of 99% and 1% of unidentified material. Fig. 12B shows the EDS elemental analysis results of a section of the sample. Showing a high intensity peak for Al and two smaller peaks for O and Si. The peak shown for C corresponds to the conductive graphite C coating used for the analysis. The elemental percentages obtained from the EDS analysis were 98.74% Al, 0.84% O, and 0.42% Si.

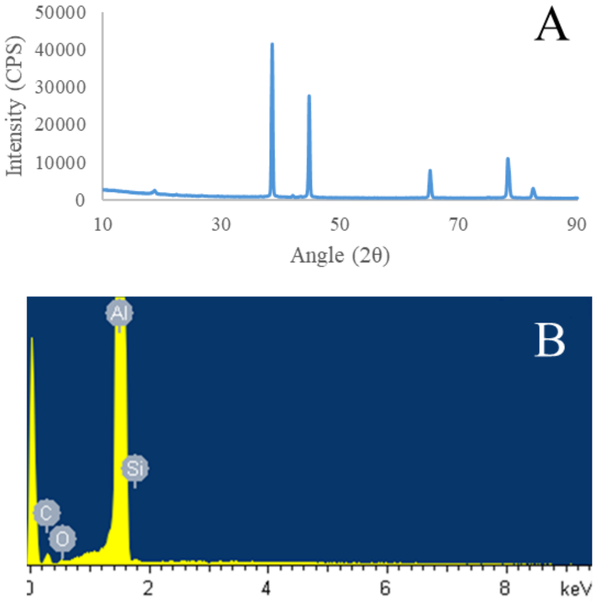

Fig. 12. Analysis results of the Al samples. Fig. 12A shows the XRD pattern obtained from the Al spherules. The characteristic peaks of Al were observed. Fig. 12B shows EDS results. Four peaks are labeled on the image: Al had the highest intensity. Si & O peaks were very small (impurities in the sample). C peak comes from the conductive graphite layer used for the analysis.

The obtained Al was processed into a wire. It was necessary to remelt the Al and cast it in a cylindrical mold. The material also had to be cold worked by hammering and then fed into a rolling machine. When the cross section was small enough, a drawing process was carried out to produce a wire. The resulting wire is shown in Fig. 13. This wire will be further tested in a 3D printing process using EBAM, a technique well suited for the moon.

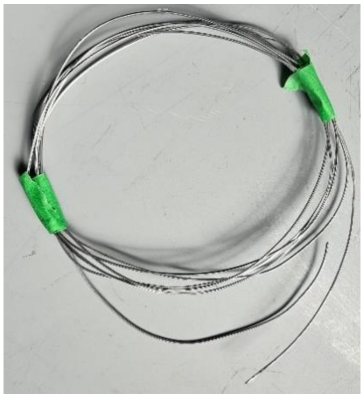

Fig. 13. Shows the Al wire made from the reaction products. It is shown that it was possible to make a spool with this wire.

1.3 Electrolysis of an LHS-1 simulant.

The latest efforts have been focused on the use of a basket type electrode to directly electrolyze a sample of a beneficiated lunar highlands regolith simulant by magnetic separation (removing the Fe fraction). The basket electrode had a mesh size fine enough to not allow any regolith particles to pass through it. The basket electrode that was tested for the experiments was made of stainless steel and the parameters used were the most successful ones for the electrolysis of pure Al_2O_3 using a rod-type electrode. The objective was to determine if it is possible to obtain Al or any other elements present in the anorthite separately, or if just a mongrel alloy containing these elements would be obtained. In case of the latter, it may be useful to evaluate if this alloy could be useful for a sustained presence on the Moon. The use of this type of electrode provided valuable insights. First, its capability of retaining samples with a small particle size at a temperature of 950°C was confirmed (Fig. 14).

Fig. 14. Beneficiated LHS-1 held by the basket electrode at 950°C. The figure shows the electrode after being temporarily taken out of the reactor. The beneficiated LHS-1 can be seen as a red hot material retained by the electrode basket.

Secondly, it was determined that the larger contact surface of the basket electrode compared to the rod electrode increased the current density in the cell. As a result, a big portion of the electrolyte was electrolyzed during the first trials probably forming chlorine (Cl_2). This led to the conclusion that lower voltages and currents should be used with this type of electrode. A comparison between the amount of $CaCl_2$ at the start of the process and the resulting amount after several hours of electrolysis can be seen in Fig. 15.

Fig. 15A shows that the molten electrolyte is completely covering the basket electrode, and that the Al_2O_3 crucible is practically full. In contrast, Fig. 15B shows that most of the electrolyte disappeared after several hours of reaction. The electrode is clearly visible and only the bottom of the electrolyte is covered by the solidified electrolyte.

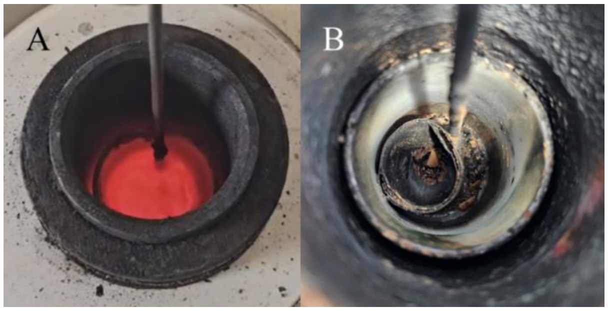

Fig. 15. $CaCl_2$ electrolyzed by the basket electrode. Fig. 15A shows the basket electrode completely immersed in the molten electrolyte. Fig. 15B shows the interior of the crucible after the reaction. Most of the electrolyte was lost, leaving the electrode visually exposed.

It was determined that stainless steel is a poor material for the cathode as any Al that is formed will immediately fuse with the Fe in the stainless steel creating an alloy, consequently damaging the electrode. This is particularly problematic in an electrode as complex as a basket electrode, where a fine mesh is used. The merging between any formed Al and the stainless steel in the electrode creates increasingly larger openings through which the particles of the reagent used (in this case the LHS-1 beneficiated simulant) will pass through avoiding the reaction. The above mentioned phenomena are shown on Fig. 16.

Finally, it was possible to reduce some of the particles present in the beneficiated LHS-1. Fig. 17 shows the physical appearance of the reaction products. Most of the product consisted of a black powder. A distinctly colored fraction of particles with a metallic appearance is also shown which corresponds to the reduced material.

Fig. 16. Fusing observed between the basket electrode and the products from the electrolysis of a beneficiated sample of LHS-1.

Fig. 17. Powdered products obtained from the electrolysis of an LHS-1 sample. Two main phases were observed: a fine black powder and bigger particles with a metallic finish.

The reaction products were imaged by SEM and analyzed by EDS to qualitatively identify the elements present in the particles with a metallic finish. Fig. 18 shows one of the particles observed by this type of microscopy and the major elements detected by EDS mapping. Fig. 18A shows an image of the analyzed particle. It is possible to notice that the analyzed particle has a fissure in its center where particles of smaller dimensions entered. Fig. 18B shows the location of Si in the sample. Si is practically absent in the sample, being found only in the upper right corner as part of the fine powder. Anorthite contains Ca, Al, Si, and O. Not finding Si is promising as it would seem that there is a mechanism through which this element can be separated from other relevant elements such as Al and Ca. Fig. 18C shows that the surface of the largest particle is mainly composed of Al. O was hardly detectable in this sample and therefore was not mapped, which would suggest that the Al detected is in its elemental form or in the form of an alloy with chromium (Cr), Fe, and Ca. Lastly, Fig. 18D shows the combination of the mappings obtained for Cr, Fe, and Ca. The brightest points correspond to Cr and Fe, while the dimmest points correspond to Ca.

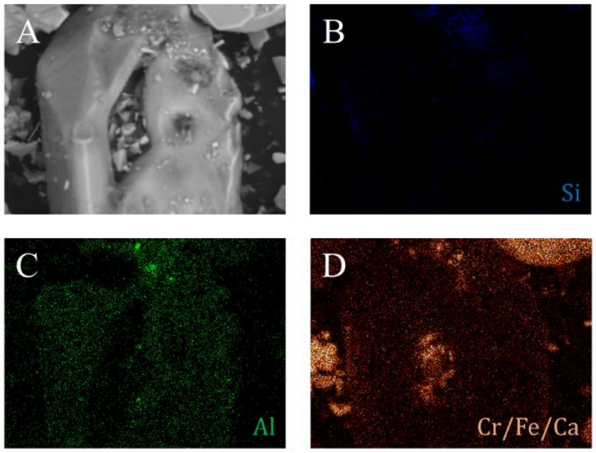

Fig. 18. SEM imaging and EDS mapping of the different elements detected in one of the product particles. Fig. 18A shows an SEM image of the analyzed particle. Fig. 18B shows the Si mapping in the sample, which is barely visible in the upper right corner. Fig. 18C shows the Al mapping in the samples, which is present across the particle surface. Fig. 18D shows the combination of the mappings obtained for Cr, Fe, and Ca. The material embedded in the fissure and the powder surrounding the analyzed particle was mainly made from these elements.

It is shown that the small particles embedded in the fissure of the analyzed particle are composed mainly of these heavier elements. Likewise, most of the particles surrounding the larger particle are also made of these elements. Cr and Fe probably originate from the flaking of the retort walls, product of the high temperatures at which the process operates. The surface of the large particle also contains Ca. This element was probably reduced during the electrochemical process and it's most likely forming an alloy with Al. It's also possible that this Ca comes from the electrolyte. However, this is less likely because the sample was rinsed several times with deionized water to remove any salt. Further testing will be done using different cathode materials that do not interact with the Al produced and by decreasing the voltage to prevent the electrolysis of the electrolyte.

4. Conclusions

It was demonstrated that the second stage required to produce Al from a lunar highlands' regolith simulant (LHS-1) is successful. It was shown that it is possible to electrochemically reduce Al_2O_3 to Al metal by a MSE process based on the FFC process. In this work most of the adaptations made to the reactor to achieve a successful process have been described: the use of a cooling system, the conditions required to dehydrate the $CaCl_2$ used as electrolyte, the use of stainless steel as a support for graphite on the anode to prevent it from breaking, the use of a solid reagent pellet and the importance of having a wide opening to facilitate the diffusion of the O^{2-} ions out of the cathode, the management of the voltages used and the use of conductive graphite and Ca as additives for the electrolyte. The continuous improvement of Al_2O_3 deoxidation to metallic Al through the modified parameters was also shown. Al spherules with a purity of around 99% were obtained according to XRD and EDS analyses. The casting, forging, rolling and drawing of the obtained Al yielded a wire that will be further tested on EBAM. The use of an inert anode to produce O_2 instead of C oxides has yet to be tested for this Al production method. The feasibility of this method should also be tested under conditions closer to the lunar environment. For example, by performing the reaction under vacuum or in low gravity conditions.

In this work results using a basket electrode to electrolyze a beneficiated sample of LHS-1 have also been presented. It was shown that due to having a larger contact surface in comparison to a rod electrode, the current density was significantly higher resulting in the electrolytic loss of the electrolyte. It was determined that stainless steel has a poor performance in this type of electrodes as any produced Al will immediately fuse with Fe creating openings through which the reagent particles can go through. Finally, we showed that some particles in the beneficiated LHS-1 were successfully reduced by using this type of electrode. The results of an EDS mapping showed the presence of particles composed mainly of Al lightly combined with Ca, with a practically null amount of oxygen and a minimum silicon content. Further experiments need to be carried with this type of electrode. An electrode made with a material that does not interact with the Al produced should be tested. Testing the reaction under low voltages would be important to prevent the loss of the electrolyte.

Acknowledgements

Carleton University's Machine Shop team deserves special thanks for helping with the manufacturing of critical components of the electrochemical reactor. Particular thanks to Brian Koren for reviewing the CAD designs and Nick Thomas for the machining of the parts. Most sincere gratitude to Javad Gholipour, Sheida Sarafan, and Xavier Pelletier for their constant feedback aimed at improving the quality of Al and the wire drawing process. Their efforts were critical to produce a wire that can be used on EBAM. This research received funding support from the National Research Council Canada (Grant # INBR4-000716-1).

5. References

[1] J. Papike, L. Taylor and S. Simon, "Lunar Minerals," in *Lunar sourcebook : a user's guide to the Moon*, New York, United States of America, Cambridge University Press, 1991, pp. 121-135.

[2] A. Franknoi, D. Morrison and S. Wolff, "The Lunar Surface," in *Astronomy*, Florida, USA, University of Central Florida, 2017.

[3] S. S. Schreiner, L. Sibille, J. A. Dominguez, J. A. Hoffman, G. B. Sanders and A. H. Sirk, "Reactor, Development of a Molten Regolith Electrolysis," in *8th Symposium on Space Resource Utilization*, Miami, Florida, USA, 2015.

[4] P. A. Burke, M. E. Nord, C. A. Hibbitts and J. R. Berdis, "Modeling electrolysis in reduced gravity: producing oxygen from in-situ resources at the moon and beyond," *Frontiers in Space Technologies*, pp. 1-15, 2024.

[5] Y. Peng, H. Tang, B. Mo, X. Zeng and B. Miao, "Influencing factors for the preparation of Fe0 in lunar soil simulant using high-temperature carbothermic reduction," *Advances in Space Research*, no. 70, pp. 3220-3230, 2022.

[6] F. Ballentine, M. E. Lewellyn and S. Moffatt, "Red Mud Flocculants Used in the Bayer Process," in *Essential Readings in Light Metals*, Springer, 2016, pp. 425-430.

[7] B. Thibodeau, X. Walls and A. Ellery, "Extraction of Silica and Alumina from Lunar Highland Simulant," in *ASCE Earth and Space 2024*, Miami, Florida, USA, 2024.

[8] H. Veldhuyzen, "Aluminum Extraction from an Ontario Calcic Anorthosite by Acid Processes and Resultant Products - Aluminum Chemicals, Coatings, Fillers, Absorbent, and Cement Additive," Ontario Geological Survey, Sudbury, Ontario, Canda, 1995.

[9] G. C. Chen, D. J. Fray and T. W. Farthing, "Direct electrochemical reduction of titanium dioxide to titanium in molten calcium chloride," *Nature*, vol. 407, p. 361–364, 2000.

[10] A. Ellery, "Sustainable in-situ resource utilization on the moon," *Planetary and Space Science*, vol. 184, p. 10870, 2020.

[11] A. Ellery, I. Mellor, P. Wanjara and M. Conti, "Metalysis Fray Farthing Chen Process As a Strategic Lunar In Situ Resource Utilization Technology," *New Space*, vol. 10, no. 2, pp. 224-238, 2022.

[12] B. A. Lomax, M. Conti, N. Khan, B. N. S., A. Y. Ganin and M. D. Symes, "Proving the viability of an electrochemical process for the simultaneous extraction of oxygen and production of metal alloys from lunar regolith,"

Planetary and Space Science, vol. 180, p. 104748, 2020.

[13] G. Chen and D. Fray, ""Voltammetric Studies of the Oxygen-Titanium Binary System in Molten Calcium Chloride"," *Journal of The Electrochemical Society*, vol. 149, p. E455, 2002.

[14] X. Walls, A. Ellery, P. Wanjara and K. Marczenko, "Laboratory Demonstration of Aluminium Metal Extraction from a Lunar Highland Simulant using Electrochemistry," in *ASCE Earth & Space*, Miami, Florida, USA, 2024.

[15] R. Phillips, F. J. Vastola and P. L. Walker Jr., "Factors affecting the product ratio of the carbon-oxygen reaction—II. Reaction temperature," *Carbon*, vol. 8, no. 2, pp. 205-210, 1970.

[16] H. Kadowaki, Y. Katasho, K. Yasuda and T. Nohira, "Electrolytic Reduction of Solid Al2O3 to Liquid Al in Molten CaCl2," *Journal of The Electrochemical Society*, vol. 165, no. 2, pp. D83-D89, 2018.

[17] K. S. Mohandas and D. F. Farthing, "FFC Cambridge Process and Removal of Oxygen from Metal-Oxygen Systems by Molten Salt Electrolysis: An Overview," *Transactions of the Indian Institute of Metals*, vol. 57, no. 6, pp. 579-592, 2004.